To cite this article: Uzunget SC, Erturk ZK, Baran T, Baglan Uzunget S. Usefulness of thoracic ultrasound with an ımage processing method in the diagnosis of silicosis disease. Turk J Clin Lab 2022; 3: 308-315.

Original Article

Usefulness of thoracic ultrasound with an image processing method in the diagnosis of silicosis disease

Silikozis hastalığı tanısında toraks ultrasonu ve görüntü işleme yöntemi kullanımı

Sinan Cem Uzunget*[1], Zamir Kemal Ertürk[2], Tarik Baran[3], Sezen Baglan Uzunget[4]

[1]Health Unit, Erkunt Sanayi, Ankara, Turkey
[2]Etimesgut State Hospital, Department of Emergency Medicine, Ankara, Turkey
[3]Osmaniye Korkut Ata University, Department of Civil Engineering, Osmaniye, Turkey
[4]Liv Hospital, Department of Cardiology, Ankara, Turkey

Abstract

Aim: The diagnosis of Silicosis Disease is based on regular follow-up, including physical examination, anamnesis and imaging methods, chest radiography and high resolution computed tomography (HRCT) which are the main imaging modalities shaped by universal guidelines. Due to its advantages such as rapid results, non-invasiveness, less cost of the procedure and radiation safety, thoracic ultrasound is an imaging method that can be utilized in the diagnosis of lung consolidation and alveolar-interstitial diseases and is preferred progressively. The thoracic ultrasound may accelerate the diagnostic process, with unbiased measurements, and contribute to control the disease progression by providing early diagnosis for patients with silicosis.

Material and Methods: We enrolled 34 patients with silicosis who had 1/0 or more involvement in chest radiography according to the ILO Pneumoconiosis reading score and age-matched 16 healthy volunteers. Then, pleural thickness, diaphragmatic thickness, pleural plaque, B line evaluated by thoracic ultrasound and the number of hyperechoic nodules that obtained from image processing by ImageJ Software.

Results: There were no B lines in any study groups. Moreover, the pleural and diaphragmatic thicknesses and were not different between groups.

Conclusion: It was not accomplished to convert nodular structures in the thorax ultrasound into visible graphics by the image processing method, apart from a few exceptional cases.

Keywords: Silicosis; thoracic ultrasound; image processing; pneumoconiosis

Corresponding author*: Sinan Cem Uzunget, Health Unit, Erkunt Sanayi, 1.Organize Sanayi Bölgesi Batıhun Caddesi No:2 Sincan/Ankara, TURKEY
E-mail: suzunget@yahoo.com, sinan.uzunget@erkunt.com.tr
ORCİD: 0000-0002-7945-0113
DOİ: 10.18663/tjcl.1132243
Recevied: 17.06.2022 accepted: 05.09.2022

TJCL Volume 13 Number 3 p: 308-315

Öz

Amaç: Silikozis Hastalığında Tanı, evrensel kılavuzlarla belirlenmiş, fizik muayene, anamnez ve görüntüleme yöntemlerini içeren düzenli takip ve kontrollere dayanmaktadır. Göğüs radyografisi ve yüksek çözünürlüklü bilgisayarlı tomografi (HRCT) silikozis hastalığının değerlendirilmesi için kullanılan temel görüntüleme yöntemleridir. Toraks ultrasonu pnömotoraks, akciğer konsolidasyonu, alveolar-interstisyel hastalıklar ve plevral effüzyon tanısında kullanılabilen ve hızlı sonuç alınması, non-invaziv olması, işlem maliyetinin daha az olması ve radyasyon güvenliği gibi avantajları sayesinde giderek daha çok tercih edilen bir görüntüleme yöntemidir. Silikozis hastalığı tanısında, Toraks Ultrasonu kullanılması, tanı sürecinin hızlandırılmasını, objektif kriterlerle tanımlanabilir hale getirilebilmesini ve erken tanı konulmasını sağlayarak hastalık ilerlemesinin önlenmesine olanak verebilir.

Gereç ve Yöntemler: Çalışmaya ILO Pnömokonyoz okuması sonucunda 1/0 ve daha fazla tutulum gösteren silikozis takipli 34 hasta dahil edilmiştir. Kontrol grubu olarak 16 sağlıklı gönüllünün Toraks Ultrason incelemesi yapılmış ve PA Akciğer grafilerinin ILO okuması yapılmıştır. İncelemelerde plevral kalınlık, diaphragma kalınlığı, plevral plak, B çizgisi ve görüntü işleme sonucunda ortaya çıkan hiperokojen nodüllerin sayımı değerlendirilmiştir.

Sonuç: Hiçbir inceleme grubunda patolojik sayıda B çizgisi saptanmamıştır. Gruplar arası plevral kalınlıklarda ve diafragma kalınlıklarında anlamlı bir fark gözlenmemiştir. Görüntü işleme yöntemi ile yapılan sayımlarda gruplar arasında anlamlı fark saptanmamıştır.

Tartışma: Sonuç olarak toraks ultrasonu ve ardından yaptığımız görüntü işleme metodu ile nodüler yapıların direkt olarak görünür hale gelmesi istisnai birkaç vaka dışında mümkün olmamıştır.

Anahtar Kelimeler: Silikozis; toraks ultrasonu; görüntü işleme yöntemi; pnömokonyozis

Introduction

Silicosis is an occupational lung disease caused by breathing silica dust which induces inflammation and fibrosis in the lung. The intensity and the duration of the dust exposure are main factors in this process [1, 2]. Moulding work, ceramic production, stone bench manufacturing, mining industry, rock drilling, chipping, tunneling, sandblasting, asphalt, concrete and brick cutting works are related fields where silica exposure is inevitable. Although the actual prevalence of the disease is unknown, it is stated that 30-50% of workers who work in those fields are affected by silicosis or other pneumoconiosis in the developing countries [3]. Moreover, 21488 people died due to pneumoconiotic dusts in 2016 according to the WHO Global Burden of Disease Data [4].

Consistent inhalation of silica crystalline results in diffuse pulmonary interstitial fibrosis of which effective treatment has not been defined yet. By virtue of the fact that the poor clinical course and the lack of appropiate treatments, early diagnosis is vital to control the disease [5]. Owing to its availability, chest radiography is the first line imaging modality [6]. Although most of the patients with silicosis can be detected by chest radiography, HRCT is superior to direct radiography in cases with parenchymal, airway and pleural abnormalities.

The ILO (International Labor Organization) International Pneumoconiosis Radiography Classification reading system was proposed by the ILO in order to provide a standard in the diagnosis and follow-up of silicosis and its revised version (2011) is still utilized all over the world. To attain a standard approach, opacities according to their shape and size, the affected areas in the paranchym, pleural thickness, pleural plaques, calcification and costophrenic angle obliteration are evaluated by this method. In the literature, it has been reported that there is a significant correlation between HRCT and this method [7, 8].

Examination of the thorax with USG is possible. However, this evaluation is limited by acoustic shadows of the bone structures surrounding the thorax, such as the scapula and ribs and the air that does not transmit ultrasound waves through the lung tissue well. The air-filled structure of the lung, the chest wall and the pleura create the differences among acoustic impedance, causing all ultrasound waves to be reflected. For this reason, solely the region just below the pleural surface can be visualized by USG but not the lung parenchyma. However, to increase the image quality is possible by using digital image processing methods which can suppresse image noise, dead pixels and radiographic image quality can be improved with various manipulations without changing the raw data [9, 10].

TUS emerges as an easy-to-apply alternative imaging modality to diagnose and to follow up. We hypothesize that, the usage of TUS in the diagnosis of silicosis disease will enable early diagnosis by accelerating the diagnostic process, by making the disease more identifiable with more objective criteria, reducing labor loss with its safe, economic, and easy application.

Material and Methods

A total of 50 workers from a foundry factory were included in this case control study. Working time of the workers in the foundry

industry ranged from 5 years to 23 years. We enrolled 34 male who diagnosed silicosis disease by a blinded pneumoconiosis reader and 16 healthy volunteers who had normal X-Ray reports according to ILO standards. TUS examinations were performed in all participants by a blinded investigator as well. Ethics committee approval was obtained and the study complied with the Declaration of Helsinki (Private Ankara Umut Hospital Ethical Committee- MM 2019/253).

In the ILO reading for silicosis, opacities were evaluated as small and large opacities, and small opacities (p/, q/, r/, s/, t/, u) were categorized and examined considering their size and shape. The first symbol represented the most intensely detected appearance, and the second one indicated the second most frequently detected appearance. Then, depending on the density of the small opacities, the reading results were given by dividing them into 12 more subcategories and specifying them as 0/, 1/, 2/, 3/. The second value was the category in which the reader recognized the opacity density as close [11].

Terason brand, Usmart 3200T model ultrasound was applied with Linear Probe (4-15 MHz). In the TUS, images taken from a total of 12 bilateral points were recorded (Upper Blue, Lower Blue, Phrenic Point, PLAPS Point, Upper Prone and Lower Prone) and nodules, pleural thickness and diaphragmatic thickness were measured directly. While performing a TUS, we followed some fixed points which were upper and lower blue points, lower and upper prone points, phrenic points and PLAPS points. Firstly, Upper Blue point; the operator placed his hand, named the upper blue hand, parallel to the clavicle, fingertips should be in the midline, thumbs should not be included in the measurement when taking measurements. While adjusting the operator's hand and the patient's that should be approximately the same size. Subsequently, the operator placed the other hand, called the lower blue hand, parallel and adjacent to the first hand. In brief; the midpoint of the upper hand was the upper blue point and the midpoint of the lower hand was the lower blue point. Next, the point where the transverse line drawn from the lower blue point intersected with the posterior axillary line was labelled the PLAPS point. The phrenic line was the lower border of the lower blue hand where the lung ended and the phrenic point was defined where this line intersected with the mid-axillary line. Finally; the upper prone point was the intersection between paravertebral line and the medial midline of the scapula, and the lower prone point was at the point where the paravertebral line crossed the lower point of the scapula [12,13,14]. Moreover, we assessed parenchyma directly and calculated the thicknesses of pleura and diaphragm.

We utilized ImageJ software that enabled us to process USG images [15]. Scars ranging in size from 1µm2 to 1.5 cm2, in the images taken from different parts of the lung were counted and their areas were figured as the total number, average size and the ratio of the particles to areas. 12 ultrasound images of 50 subjects were scrutinized at the original contrast level, and a total of 600 images were treated. The image processing steps were initiated with the distinguishing the image obtained from the USG device was in 8-bit format or not, and those whose image format was different from 8-bit were corrected to 8-bit later on. Then, USG images were synchronized by scaling ImageJ with the help of the ruler on it. Thus, the correct spotting of the measured magnitude on the original image by ImageJ was ensured. In the next step, the image was transformed to binary format and the images were encoded as "1" and "0" on the basis of binary coding. In the original image, the white and near-white region pixels turned black in the processed image, while the darker black toned region pixels were encoded as white (See Figures 1a and 1b). In order to avoid the reflection effects that would occur on the original images, the shapes consisting of black pixels that remained half an inch below the pleura and within a 1×2 cm rectangle in the probe imaging area were counted as particles and their sizes were determined by ImajeJ (Figure 1c).

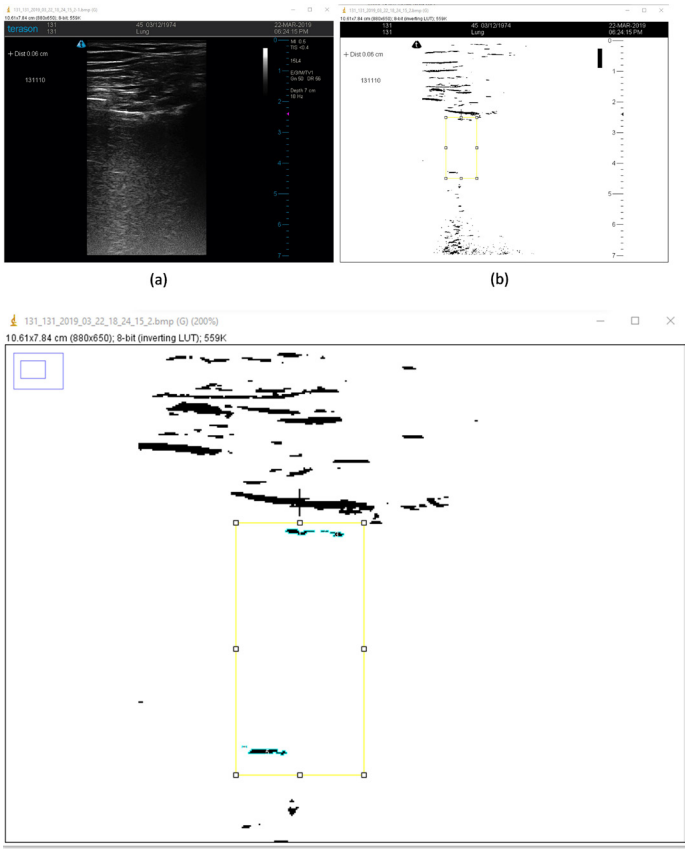

Figure 1a. Sonoghraphic image, **1b.** Image transformed to binary format, **1c.** Rectangle which pixels counted in

Statistical Analysis

The data were compared with hypothesis tests according to whether they were normally distributed or not (Kolmogorov-Smirnow/Shapiro-Wilk tests), and statistical significance was evaluated according to these results. The Mann-Whitney U test was used to compare two independent groups in data that did not illustrate normal distribution. Demographic information of the patients was presented and the data were given as mean, median, standard error, 25th percentile and 75th percentile.

Results

The study included 34 patients who diagnosed as silicosis with 1/0 or more involvement in the ILO Pneumoconiosis reading and 16 healthy individuals as control group. The patient group was evaluated in terms of involvement, 6 patient was evaluated 1/0, 16 patient was evaluated 1/1, 5 patient was evaluated 1/2, 3 patient was evaluated 2/1, 3 patient was evaluated 2/2, 1 patient was evaluated 3/3 (Table 1). TUS and the processed images by ImageJ software were obtained.

Table 1. Patient groups

	1/0	1/1	1/2	2/1	2/2	3/3
p/p	1	3	1			
p/q				1		
p/s	3	7	2	1		
q/p			1			
q/q			1		1	
q/r						1
q/t		1		1	2	
s/p	1	2				
s/s		1				
s/t	1	1				
t/q	1					

No difference was detected between the two groups in terms of their age, height and weight (p = 0.917, p = 0.983, p = 0.261, respectively) and B lines were not observed in any study groups. Furthermore, no significant difference was found at any point where pleural thicknesses were measured (Upper BLUE point right p = 0.268, Upper BLUE point left p = 0.431, Lower BLUE point right p = 0.899, Lower BLUE point left p = 0.396, Phrenic point right p= 0.774, Phrenic point left p = 0.148, PLAPS point right p = 0.767, PLAPS point left p = 0.517, Upper prone point right p = 0.139, upper prone point left p = 0.589, lower prone point right p = 0.799, lower prone point left p = 0.743) (Table 2).

Table 2. Pleural thickness

Pleural thickness	groups	mean	std. Error	25. percentil	median	75. percentil	p value
Upper Blue Point Right	Control	0,08	0,01	0,07	0,08	0,1	0,268
	Patient	0,07	0,01	0,07	0,08	0,09	
Upper Blue Point Left	Control	0,07	0,01	0,04	0,07	0,1	0,431
	Patient	0,06	0,01	0,01	0,07	0,09	
Lower Blue Point Right	Control	0,07	0,01	0,06	0,08	0,1	0,899
	Patient	0,07	0,01	0,06	0,08	0,09	
Lower Blue Point Left	Control	0,06	0,01	0,01	0,07	0,11	0,396
	Patient	0,07	0,01	0,07	0,08	0,09	
Phrenic Point Right	Control	0,07	0,01	0,01	0,08	0,1	0,774
	Patient	0,07	0,01	0,06	0,07	0,08	
Phrenic Point Left	Control	0,06	0,01	0,01	0,07	0,08	0,148
	Patient	0,07	0,01	0,06	0,08	0,09	
PLAPS Point Right	Control	0,07	0,01	0,04	0,08	0,09	0,767
	Patient	0,07	0,01	0,07	0,08	0,09	
PLAPS Point Left	Control	0,07	0,01	0,01	0,07	0,08	0,517
	Patient	0,07	0,01	0,01	0,08	0,09	
Upper Prone Point Right	Control	0,09	0,01	0,07	0,1	0,11	0,139
	Patient	0,07	0,01	0,01	0,08	0,11	
Upper Prone Point Left	Control	0,08	0,01	0,07	0,09	0,11	0,589
	Patient	0,07	0,01	0,01	0,08	0,11	
Lower Prone Point Right	Control	0,07	0,01	0,01	0,08	0,11	0,799
	Patient	0,07	0,01	0,01	0,08	0,09	
Lower Prone Point Left	Control	0,08	0,01	0,07	0,09	0,11	0,743
	Patient	0,07	0,01	0,07	0,08	0,09	

Likewise, diaphragma thickness and total count were similar (p = 0.622, p = 0.739, respectively) (Table 3) and processed images by ImageJ were not distinctive (Upper BLUE point right p = 0.325, Upper BLUE point left p = 0.745, Lower BLUE point right p = 0.58, Lower BLUE point left p = 0.115, Phrenic point right p = 0.808, Phrenic point left p = 0.519, PLAPS point right p = 0.542, PLAPS point left p = 0.234, Upper prone point right p = 0.227, upper prone point left p = 0.402, lower prone point right p = 0.254, lower prone point left p = 0.913) (Table 4).

Table 3. Diaphragma thickness and total count

	groups	mean	std. eror	25. percentil	median	75. percentil	p value
Diaphragma thickness	Control	0,19	0,02	0,15	0,17	0,19	0,622
	Patient	0,18	0,01	0,16	0,17	0,21	
Total Count	Control	110,88	45,499	27,5	53,5	98,5	0,739
	Patient	127,94	27,865	24	61	167	

Table 4. Counted points after processing image

	groups	mean	std. Error	25. percentil	median	75. percentil	p value
Upper Blue Point Right	Control	7,31	5,14	0	0,5	3	0,325
	Patient	9,06	2,85	0	2	6	
Upper Blue Point Left	Control	10,31	6,8	0	1,5	7,5	0,745
	Patient	9,15	3,54	0	1	3	
Lower Blue Point Right	Control	24,38	9,82	0	3,5	36	0,58
	Patient	19,53	5,01	2	7	23	
Lower Blue Point Left	Control	11,63	4,29	1	4	13,5	0,115
	Patient	26,68	5,65	2	14	37	
Phrenic Point Right	Control	9,25	3,49	0	5	12,5	0,808
	Patient	10,15	2,73	0	2	15	
Phrenic Point Left	Control	3,56	2,06	0	1	2	0,519
	Patient	11,41	4,34	0	1,5	7	
PLAPS Point Right	Control	16,38	7,98	0,5	3	6,5	0,542
	Patient	16,38	4,99	0	5,5	13	
PLAPS Point Left	Control	8,06	5,08	0	1,5	4	0,234
	Patient	11,65	3,73	1	3	13	
Upper Prone Point Right	Control	4,75	4,62	0	0	0	0,227
	Patient	5,26	2,39	0	0	1	
Upper Prone Point Left	Control	6,38	5,66	0	0	0,5	0,402
	Patient	4,47	1,95	0	0	2	
Lower Prone Point Right	Control	2,56	1,69	0	0	0,5	0,254
	Patient	1,12	0,67	0	0	0	
Lower Prone Point Left	Control	6,25	6,05	0	0	0	0,913
	Patient	4,12	2,48	0	0	0	

Discussion

In the current report, we analyzed 34 patients with silicosis and 16 healthy foundry workers by TUS and an image processing method. We could not illustrate B lines and no significant difference between pleural and diaphragmatic thicknesses and in the analysis generated by the image processing method in any study groups.

Dust protection is essential to prevent from silicosis and this basically contains two approaches which can be summarized as inhibiting dust at the source and using personal protective equipment [16]. Still, vigorous preventive efforts should be considered such as regular medical follow-up, pulmonary function tests and chest X-ray of those exposed to crystalline silica to identify the disease before the clinical picture emerges. When silicosis is suspected in the periodical examinations or as a result of the ILO evaluation, patients are referred to the relevant clinic for detailed exploration such as HRCT. However, those procedures have handicaps in terms of bearing radiation exposure, loss of time and labor and high cost.

In our study, to simplify this course, we intended to uncover lung and pleural signals that may rise in silicosis by using TUS and compared them with the ILO evaluation. In the literature, there are some promising results exemplifying the lung parenchymal diseases by TUS. Even though we did not show significant differences among parenchyma images, pleura and diaphragm thicknesses, some studies that compared TUS and HRCT in patients with alveolar-interstitial syndrome, illustrated existing alveolar consolidation by TUS [17, 18]. Additionally, two studies proposed that TUS could be utilized for evaluation of the thorax in intensive care [13, 19] and the emergency department [20]. Although it was not statistically significant, in some of our cases, hyper echogenic appearances were obtained by TUS in the lung parenchyma in which large opacities were shown in the ILO evaluations and in HRCT images as well (Figure 2).

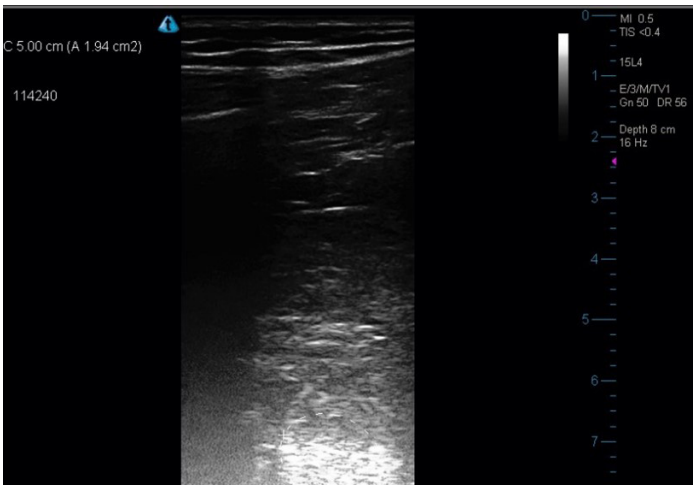

Figure 2. Hyperechoic image in lung parenchyma

Interstitial pulmonary pathologies consist of a heterogeneous group of disorders that involve the pulmonary interstitium and lead to impaired gas exchange. As the fluid content of the lung expands and the air in the alveoli shrinks, the fluid accumulates in the interstitial and alveolar space. As a result, a number of vertical, hyperechoic so-called "B-lines" are appeared in the USG. In fact these are sorts of reverberation artifacts caused by the reflection of ultrasound waves at the interlobular septa and these images are seen as vertical, hyperechoic, laser-beam-like lines with sharp edges that start from the pleural line and continue to at the end of the ultrasound screen [21, 22]. Since the parenchymal density increases in nodular opacities, we expected that a relatively hyperechogenic appearance would have been obtained as the reflection of ultrasound wave. Moreover, we assumed that the nodules could have been appeared more hyperechogenic than the surrounding tissue so the TUS could have differentiated opacities from effusion and consolidation seen on chest X-ray [23]. Unfortunately, we could not prove our hypothesis in clinical practise.

In the ILO evaluation of pneumoconiosis, pleural pathologies are classified as pleural plaque (localized pleural thickening), costophrenic angle obliteration and diffuse pleural thickening [11]. In our study, no significant difference was observed in pleural thicknesses between the volunteer group and the silicosis group. Though, in only two cases in the Silicosis group had pleural plaque, the pleural thicknesses were normal in the USG evaluation of these individuals. Diaphragmatic thickness was also contemplated to be associated with the severity of the disease in some pulmonary pathology. Previously, a significant correlation between diaphragmatic thickness and clinical parameters in COPD was outlined advocating that diaphragmatic thickness measurement by USG was a beneficial prognostic marker in the evaluation of pulmonary rehabilitation in COPD patients [24, 25]. Also, measurement of diaphragmatic thickness by USG in COPD patients has been speculated to be useful to strength the clinical decision [26]. In contrast to the studies that proposed to measure the diaphragmatic thickness by TUS [11], we did not observe any increases in diaphragmatic thickness or any other USG evidences of it.

In this study, images were altered by ImajeJ, open source software. While the spaces appeared black in ultrasound images, tissues such as bone, pleura, etc. leaved brighter traces. Accordingly, if there was nodular tissue in the lung, it left a hyperechoic scar. Since these traces could be very small and/or did not reflect sound waves fairly, it was plausible to scan them with the image processing method.

Digital image processing is utilized to suppress noise of images, to remove dead pixels and to improve radiographic image quality via various manipulations without distorsing the raw data. We presumed that we could distinguish the appearances of silica nodules, artifacts and noises observing on TUS. So we tested ImageJ which is a proven software that has been used in some scientific fields such as health and astronomy for many years [27,28]. But no statistically significant differences were achieved with this method as well.

In our study, solely pathological regions in the upper blue points where a higher number of signals increased were compatible with the ILO readings but we did not reach the same results for all these regions in patients with silicosis. Whole view of the structures in a three-dimensional form can be projected onto PA chest X-ray as two-dimensional plane, but this is not possible in USG evaluation. The images of the tissue can be reflected on the screen provided that they are on the same plane but other layers cannot be analyzed unless the angle of the probe is changed. This difference may explain the reason why pathological formations seen on PA chest X-ray but not visible on USG.

In conclusion, except for a few cases, we could not accomplish to form nodular structures to be directly obvious with the TUS and/or the image processing method.

Acknowledgment

We would like to thank Mr. Korat Kılıç, who provided us with the Terason Usmart 3200T model ultrasound device that we used in our study, without demanding any compensation.

Ethics approval

All procedures performed in studies involving human participants were in accordance with the ethical standards of the institutional and/or national research committee and with the 1964 Helsinki Declaration and its later amendments or comparable ethical standards. All persons included in the study signed the informed consent form.

Declaration of conflict of interest

The authors report that there was no funding source for the work that resulted in the article or the preparation of the article.

Authors' contributions

All authors have made substantial contributions to the conception and design of the study, acquisition of data, or analysis and interpretation; drafting the article or revising it critically for important intellectual content and final approval of the version to be submitted. All authors endorse the data and conclusions.

References

1. Fubini B, Hubbard A. Reactive oxygen species (ROS) and reactive nitrogen species (RNS) generation by silica in inflammation and fibrosis.Free. Radic. Biol. Med. 2003; 34: 1507–1516
2. Rimal B, Greenberg AK, Rom WN. Basic pathogenetic mechanisms in silicosis: current understanding. Curr. Opin. Pulm. Med. 2005; 11: 169–173
3. T.C.Sağlık Bakanlığı Sağlık Hizmetleri Genel Müdürlüğü, Pnömokonyozlarda sağlık gözetimi, klinik tanı, kayıt, bildirim ve izlem protokolü, Ankara, 2021: 5-26
4. GBD 2016 Occupational Chronic Respiratory Risk Factors Collaborators. Occup Environ Med 2020;77:142–150.
5. Alvarez RF, Gonzalea CM, Martinez AQ, Perez JJB, Fernandez LC, Fernandez AP. Guidelines for the Diagnosis and Monitoring of Silicosis, Arch Bronconeumol.2015;51(2):86-93
6. Bacchus L, Shah RD, Chung JH, Crabtree TP, Heitkamp DE, Iannettoni MD, Johnson GB, Jokerst C, Mccomb BL, Saleh AG, Steiner RM, Mohammed TH, Ravenel JG. Occupational lung disaeses, ACR Appropriateness criteria, J Thorac Imaging. 2016 Jan;31(1):W1-3
7. Ergün D, Ergün R, Evcik E, Öziş TN, Akkurt İ, The relation between the extent of radiological findings and respiratory functions in pneumoconiosis cases of dental technicians who are working in Ankara, Tuberk Toraks 2016;64(2):127-136
8. Berk S, Dogan DO, Gumus C, Akkurt I. Relationship between radiological (X-ray/HRCT), spirometric and clinical findings in dental technicians' pneumoconiosis. Clin Respir J 2016;10:67-73
9. Prokop M, Neitzel U, Schaefer-Prokop C. Principles of image processing in digital chest radiography, Journal of Thoracic Imaging, 18(3), 148-164
10. Seeram E. Digital image processing. Radiol Technol. 2004 Jul-Aug;75(6):435-52; quiz 453-5. PMID: 15352557
11. International Labour Office. Guidelines for the use of the ILO International classification of radiographs of pneumoconioses, revised edition 2011, https://www.ilo.org/global/topics/safety-and-health-at-work/resources-library/publications/WCMS_168260/lang--en/index.htm, Last Access 07/07/2022
12. Lichtenstein D, Meziere G. The BLUE-points: three standardized points used in the BLUE-protocol for ultrasound assessment of the lung in acute respiratory failure, Crit Ultrasound J 2011; 3:109–110
13. Lichtenstein D. Novel approaches to ultrasonography of the lung and pleural space: where are we now? Breathe 2017; 13: 100–111.
14. Soldati G, Smargiassi A, Inchingolo R, Buonsenso D, Perrone T, Briganti DF, Perlini S, Torri E, Mariani A, Mossolani EE, Tursi F, Mento F, Demi L. Proposal for International Standardization of the Use of Lung Ultrasound for Patients With COVID-19: A Simple, Quantitative, Reproducible Method. J Ultrasound Med. 2020 Jul;39(7):1413-1419. doi: 10.1002/jum.15285. Epub 2020 Apr 13. PMID: 32227492; PMCID: PMC7228287.
15. Imagej.nih.gov (homepage on the Internet). Imagej Image Processing and Analysis in Java, Available from: https://imagej.nih.gov/ij/ Last Access 28/10/2021
16. Leung CC, Sun yu IT, Chen W. Silicozis, Lancet 2012;379: 2008-18.
17. Stefanidis K, Dimopoulos S, Kolofousi C, Cokkinos DD, Chatzimichail K, Eisen LA, Wachtel M, Karakitsos D, Nanas S. Sonographic Lobe Locaziation of Alveolar-Interstitial Syndrome in the Critically Ill, Crit Care Res Pract. 2012; 2012: 17919
18. Volpicelli G, Caramello V, Cardinale L, Mussa A, Bar F, Frascisco MF. Detection of sonographic B-lines in patients with normal lung or radiographic alveolar consolidation, Med Sci Monit, 2008; 14(3): CR122-128
19. Lichtenstein D, Van Hooland S, Elbers P, Malbrain MLNG. Ten good reasons to practice ultrasound in critical care, Anaesthesiol Intensive Ther 2014; vol.46, no 5, 323-335
20. Wongwaisayawan S, Suwannanon R, Sawatmongkorngul S, Kaewlai R. Emergency Thoracic US: The Essentials, RadioGraphics 2016; 36:640-659.
21. Lichtenstein D, Mézière G, Biderman P, Gepner A, Barré O. The comet-tail artifact: An ultrasound sign of alveolar-interstitial syndrome. Am J Respir Crit Care Med 1997; 156: 1640-6

22. Çiftçi E, Akhun N. Ultrasonografi için temel bilgiler. Çağlayan B (Editör). Klinik uygulamada toraks ultrasonografisi. İstanbul: Probiz yayıncılık; 2010. s.1-7

23. Volpicelli G, Elbarbary M, Blaivas M, Lichtenstein DA, Mathis G, Kirkpatrick AW, Melniker L, Gargani L, Noble VE, Via G, Dean A, Tsung JW, Soldati G, Copetti R, Bouhemad B, Reissig A, Agricola E, Rouby JJ, Arbelot C, Liteplo A, Sargsyan A, Silva F, Hoppmann R, Breitkreutz R, Seibel A, Neri L, Storti E, Petrovic T. International Liaison Committee on Lung Ultrasound (ILC-LUS) for International Consensus Conference on Lung Ultrasound (ICC-LUS). International evidence-based recommendations for point-of-care lung ultrasound. Intensive Care Med. 2012 Apr;38(4):577-91. doi: 10.1007/s00134-012-2513-4. Epub 2012 Mar 6. PMID: 22392031.

24. Ogan N, Aydemir Y, Evrin T, Ataç GK, Baha A, Katipoğlu B, Süzen B, Akpınar EE, Diaphragmatic thickness in chronic obstructive lung disease and relationship with clinical severity parameters, Turk J Med Sci 2019; 49: 1073-1078

25. Crimi C, Heffler E, Augelletti T, Campisi R, Noto A, Vancheri C, Crimi N, Utility of ultrasound assesment of diafragmatic function before and after pulmonary rehabilitation in COPD patients, International Journal of COPD 2018;13: 3131-3139

26. Evrin T, Korkut S, Ozturk Sonmez L, Szarpak L, Katipoglu B, Smereka J, Guven R, Akpinar EE. Evaluating Stable Chronic Obstructive Pulmonary Disease by Ultrasound. Emerg Med Int. 2019 Sep 15;2019:5361620. doi: 10.1155/2019/5361620. PMID: 31637058; PMCID: PMC6766158.

27. Schneider CA, Rasband SR, Eliceiri KW. NIH Image to ImageJ: 25 years of image analysis, Nature methods 9, 2012; 671-675.

28. Debut A,Vizuete K, Pazmino K, Calderon J, Gallegos C, Gaona V. Effect of Visual Cognition on the Measurement of Particle Size Using ImageJ Software, Current Materials Science: Formerly: Recent Patents on Materials Science 14.2 (2021): 141-154.